Asymmetric Organocatalysis

International Edition: DOI: 10.1002/anie.201508980
German Edition: DOI: 10.1002/ange.201508980

Importance of Intermolecular Hydrogen Bonding for the Stereochemical Control of Allene–Enone (3+2) Annulations Catalyzed by a Bifunctional, Amino Acid Derived Phosphine Catalyst

*Mareike C. Holland, Ryan Gilmour, and K. N. Houk**

Dedicated to Professor Albert Eschenmoser on the occasion of his 90th birthday

Abstract: *The origin of stereoselectivity in the (3+2) annulation of allenes and enones catalyzed by an amino acid derived phosphine catalyst has been investigated by the use of dispersion-corrected density functional theory. An intermolecular hydrogen bond between the intermediate zwitterion and the enone was found to be the key interaction in the two enantiomeric transition states. Additional stabilization is provided by intermolecular hydrogen-bonding interactions between acidic positions on the catalyst backbone and the substrate. Enantioselectivity occurs because the intermolecular hydrogen bond in the transition state leading to the minor enantiomer is only possible at the expense of reactant distortion.*

Phosphines are powerful nucleophilic organocatalysts that continue to find application in the rapid construction of densely functionalized cyclic and acyclic biologically important molecules.[1] Their significance is beautifully exemplified by (3+2) annulation reactions of allenes and activated olefins or imines under the catalysis of PR_3 derivatives.[2] Since the initial report of this transformation in 1995,[2a] asymmetric variants of this reaction have been developed relatively slowly despite their potential in natural product total synthesis.[3] The seminal example of an enantioselective (3+2) annulation with an amino acid derived phosphine catalyst was reported by Cowen and Miller in 2007 (Scheme 1, top).[4] This reaction unifies simple allenoate esters and enones under the catalysis of an amino acid derived β-aminophosphine with good to excellent selectivity. Since then, several other organophosphine catalysts derived from amino acids have been reported for this and related reactions.[5,6] All these catalysts feature a hydrogen-bonding group (amide or thiourea) vicinal to a diphenylphosphine group. To delineate the interactions responsible for enantioselectivity in this important class of transformations, we studied the initial reaction reported by Cowen and Miller. The role of the functional groups and the origin of stereoselectivity in this transformation were established by computational investigation of the bond-forming steps of the reaction mechanism. Elucidation of the key stabilizing interactions in the enantiodetermining transition state will assist the development of novel organocatalysts for related transformations and assist the formulation of induction models.

The mechanism (Scheme 1, bottom) and the origins of regioselectivity of the corresponding achiral reaction with PMe_3 have been studied previously.[7] These studies have demonstrated that the catalyst initially undergoes addition to the β-position of the allenoate to give a zwitterionic species. The backbone geometry of this intermediate is rigidified by a close contact between the negatively charged oxygen atom and the phosphonium ion. To ensure that the same interaction controls the geometry of the reactive intermediate when a bulkier phosphine catalyst is used, we studied the zwitterion resulting from the addition of PPh_3 (Figure 1). The same conformation in which the negatively charged oxygen atom is located *cis* to the phosphonium moiety is lowest in energy, even though the energetic difference is slightly less than for the PMe_3 case. The addition of the catalyst to the allenoate was found to be the rate-determining step. The isomerization of *cis*/*trans* allenoates has been studied by NMR spectroscopic analysis,[8] and consistent with these experiments, it was found that the isomers are very close in energy ($\Delta\Delta G = 0.2$ kcal mol^{-1}). The barrier for the addition of PPh_3 to the *cis* allenoate is 1.3 kcal mol^{-1} lower than for addition to the *trans* allenoate (Figure 2). Furthermore, the formation of the zwitterion was found to be the rate-determining step ($\Delta\Delta G^{\ddagger} = 25.2$ kcal mol^{-1}; compare with Figure 3).

Detailed investigations of the achiral reaction have shown that the cycloaddition occurs by a stepwise mechanism. The reaction coordinate leading to both the major and the minor enantiomer with the Miller catalyst was investigated, and the first bond-forming event was identified as the enantiodetermining step in both pathways (Figure 3). A proton-transfer sequence catalyzed by trace amounts of water is likely to be responsible for elimination of the catalyst.[9]

We focused on the structural features of the transition state of the stereodetermining first step of the annulation reaction (see the Supporting Information for the energetically lowest lying conformations of the other intermediates and transition states of the reaction pathway). In their seminal

[*] Dr. M. C. Holland, Prof. Dr. K. N. Houk
Department of Chemistry and Biochemistry
University of California, Los Angeles
Los Angeles, CA 90095 (USA)
E-mail: houk@chem.ucla.edu
Dr. M. C. Holland, Prof. Dr. R. Gilmour
Organisch Chemisches Institut
Westfälische Wilhelms-Universität Münster
48149 Münster (Germany)

Supporting information for this article is available on the WWW under http://dx.doi.org/10.1002/anie.201508980.

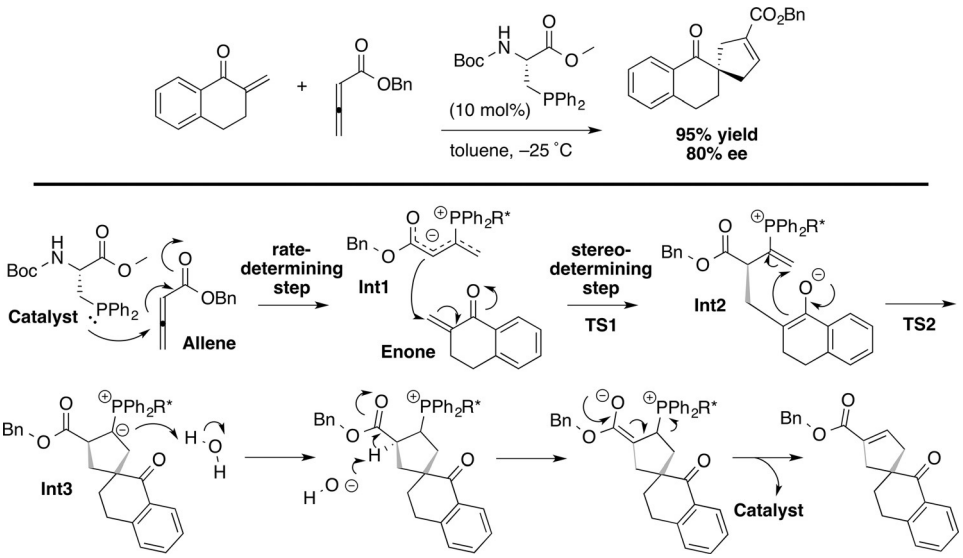

Scheme 1. Top: Asymmetric (3+2) annulation of allenoates with enones in the presence of a phosphine catalyst derived from an amino acid.[4] Bottom: Proposed mechanism based on studies by the research groups of Kwon and Yu.[7] Boc = *tert*-butoxycarbonyl, Bn = benzyl.

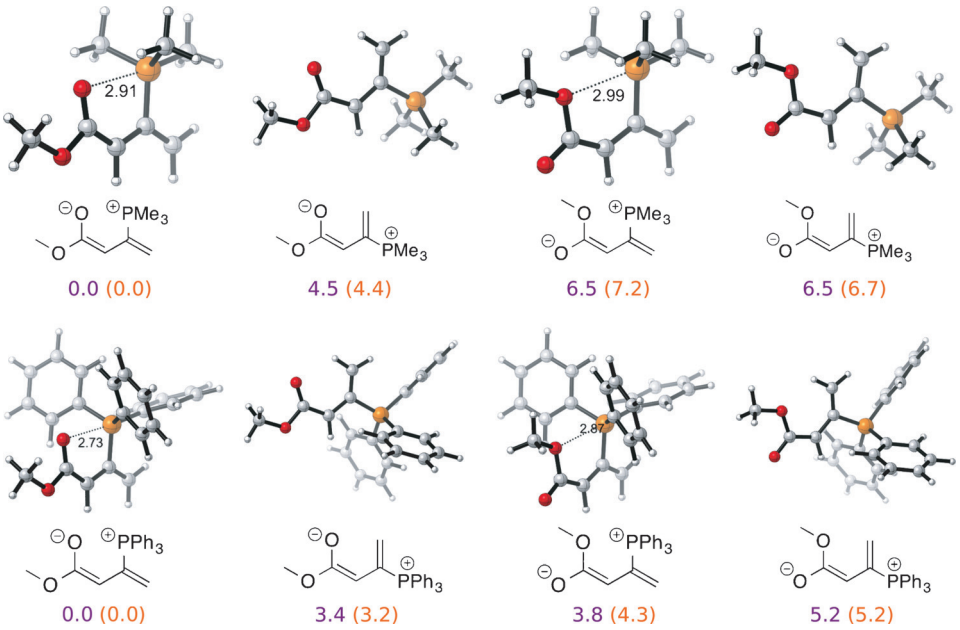

Figure 1. The intermediate zwitterion prefers a geometry that allows for a stabilizing contact between the charges, both for PMe_3 and PPh_3. Distances are given in angstroms (Å) and relative free energies ($\Delta\Delta G$) in kcal mol^{-1} (B3LYP-D3(BJ)/def2-TZVPP/IEF-PCM(toluene)//B3LYP/6-31G(d)/IEF-PCM (toluene) (M06-2X/def2-TZVPP/IEF-PCM(toluene)//B3LYP/6-31G(d)/IEF-PCM (toluene)); O red, P orange.

report, Cowen and Miller proposed a stereoselectivity model in which an intramolecular hydrogen bond is responsible for preorganizing the zwitterion in such a way that one face is blocked by a phenyl group, thus ensuring selectivity in the subsequent nucleophilic attack (Scheme 2A).[4] This model was also proposed by Zhao and co-workers for a related reaction.[6b] An alternative explanation was offered by Fang and Jacobsen for the (3+2) annulation of an imine and an allene under the catalysis of a structurally related amino acid derived phosphinothiourea.[6a] This model proposes that intermolecular hydrogen bonds form between the thiourea moiety and the substrate (Scheme 2B). Several subsequent reports have adopted one of the two models, but mechanistic proof for either proposal remains scarce. We have found only two previous computational studies on aminophosphine-catalyzed reactions. Lu, Huang and co-workers studied an aza-Morita–Baylis–Hillman reaction promoted by a catalyst related to the Miller catalyst.[10] Their study suggests that an intramolecular hydrogen bond is responsible for the high levels of stereoselectivity (Scheme 2C). In contrast, Lan, Lu, and co-workers found an intermolecular hydrogen bond to be responsible for good levels of asymmetric induction in the γ-addition of 5*H*-thiazol/oxazol-4-ones to allenoates (Scheme 2D).[11]

Our computations show that the lowest-energy transition state features an intermolecular hydrogen bond (1.92 Å, (*S*)-TS; Figure 4, top) between the carbamate and the substrate and is thus similar to the models proposed by Jacobsen and Lu (Scheme 2). Further stabilization comes from hydrogen-bonding interactions between two of the acidic hydrogen substituents α and β to the phosphonium ion (2.20 and 2.34 Å, respectively). These three noncovalent interactions efficiently bind the substrate in a chiral pocket that is reminiscent of biomolecular catalysis. Another important feature is the previously discussed rigid conformation around the zwitterionic backbone. This conformation allows for close contact between the negatively charged oxygen atom and the phosphonium ion (2.92 Å). One transition-state conformation that only differs in the positioning of the benzyl group was found to be close in energy to the discussed minimum conformation ($\Delta\Delta G^{\ddagger}$ = 0.32 (0.12) kcal mol^{-1}; see the Supporting Information). All other located conformations are >2.5 kcal mol^{-1} higher in energy. A transition state featuring an intramolecular hydro-

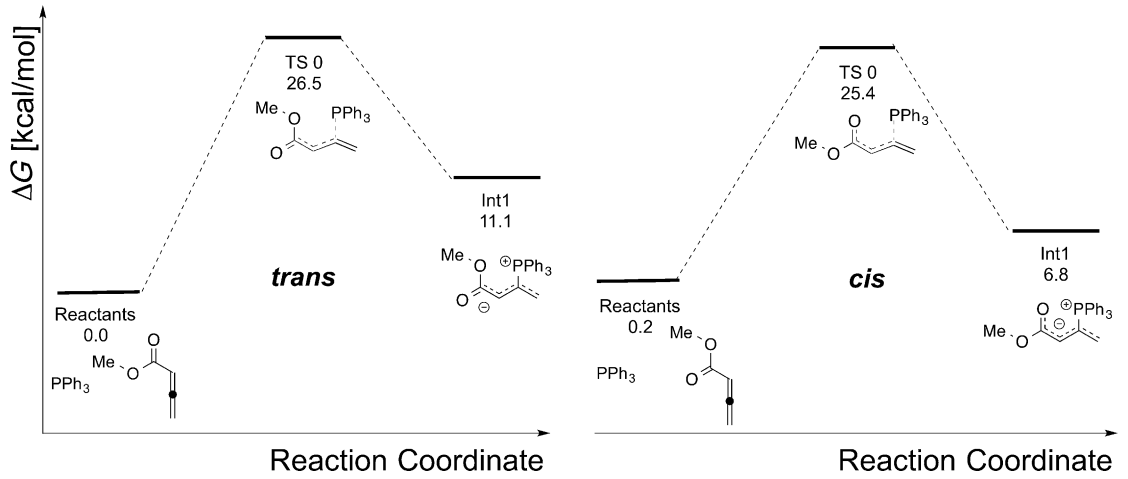

Figure 2. Addition of PPh_3 to the *trans* and *cis* allenoate. Relative free energies ($\Delta\Delta G$) are given in kcal mol^{-1} (M06-2X/def2-TZVPP/IEF-PCM(toluene)// B3LYP/6-31G(d)/IEF-PCM(toluene).

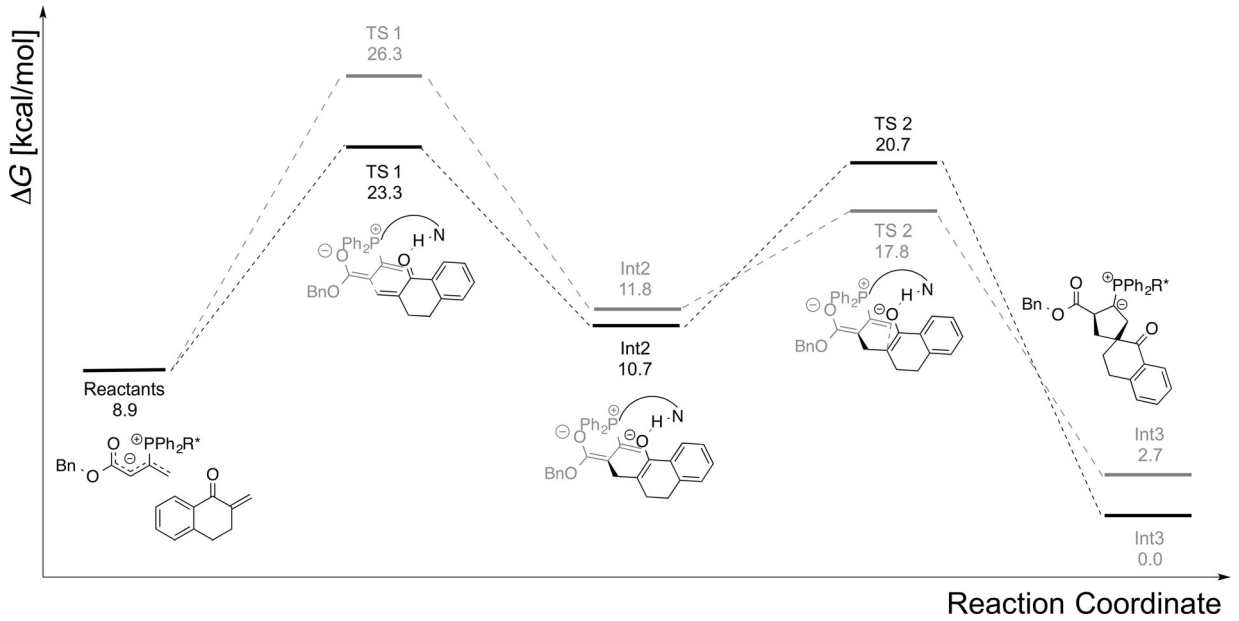

Figure 3. Free-energy reaction profile of the two bond-forming events of the (3+2) annulation reaction. The black pathway leads to the major enantiomer; the gray pathway leads to the minor enantiomer. Only structures of the major pathway are shown. Relative free energies ($\Delta\Delta G$) are given in kcal mol^{-1} (M06-2X/def2-TZVPP/IEF-PCM(toluene)//B3LYP/6-31G(d)/IEF-PCM(toluene).

gen bond (2.36 Å) as proposed by Miller and Huang (Scheme 2) was found to be 10–13 kcal mol^{-1} higher in energy ((*S*)-TS; Figure 4, bottom).

The lowest-lying transition state leading to the minor enantiomer (*R*)-TS (Figure 5) was found to be 3.0 kcal mol^{-1} higher in energy, which is in agreement with, but overestimates, the experimentally observed selectivity of 80 % *ee* at −25 °C. Like (*S*)-TS, it is preorganized by the same kind of hydrogen-bonding interactions. The considerable overestimation of selectivity can partially be explained by the existence of a number of other transition-state geometries leading to the minor enantiomer that are close in energy (eight structures within 1.5 kcal mol^{-1}; see the Supporting Information). Interestingly, some of these structures feature an intramolecular hydrogen bond similar to the key interaction proposed by Miller and Huang (see Scheme 2 and the Supporting Information).

The lowest transition states were further investigated by overlaying (*S*)-TS and (*R*)-TS along the chiral backbone and the zwitterionic moieties (Figure 6). The overlay along the zwitterion reveals that in (*S*)-TS, the chiral chain is placed over the substrate. Conversely, in (*R*)-TS, this group is rotated into a more unfavorable orientation to allow for an optimal hydrogen-bonding pattern, thus bringing the carbamate

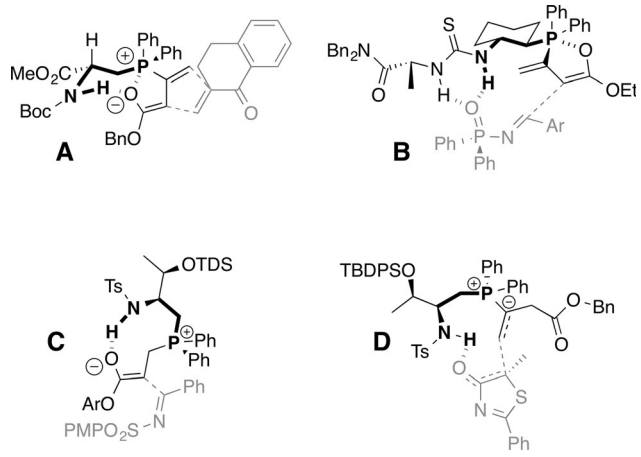

Scheme 2. Transition-state models proposed by A) Cowen and Miller, B) Fang and Jacobsen, C) Lu, Huang, and co-workers, and D) Lan, Lu, and co-workers to rationalize observed stereoselectivity.

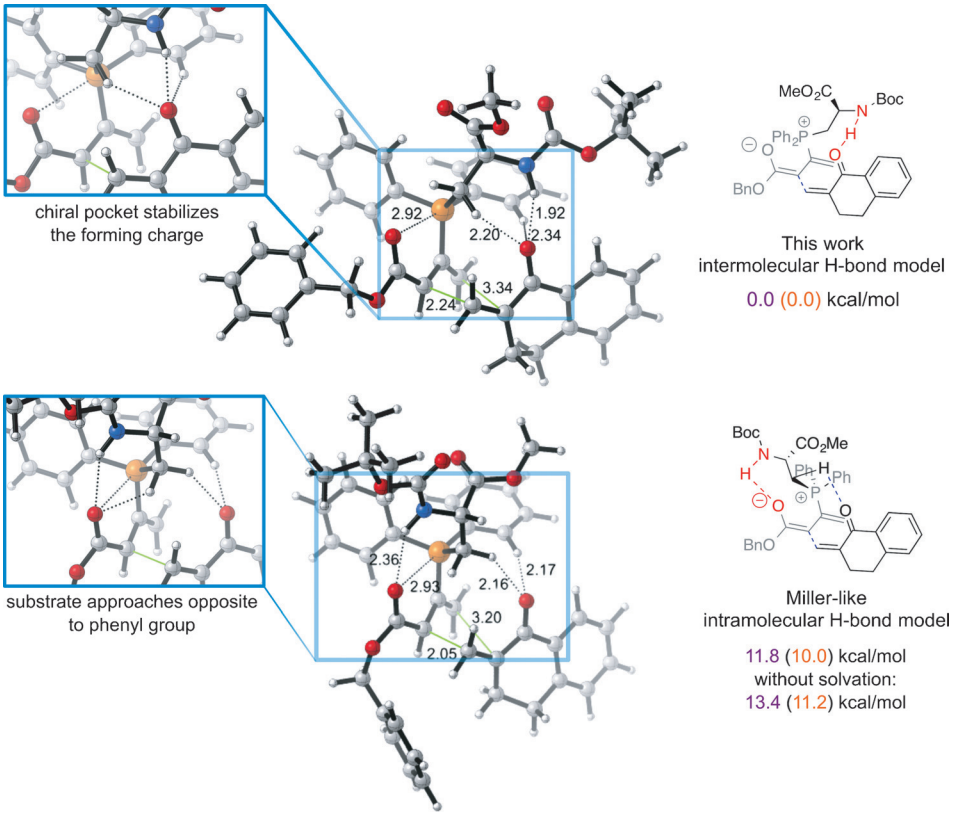

Figure 4. The transition-state model based on DFT analysis features an intermolecular hydrogen bond between the chiral chain of the catalyst and the enone. A transition state featuring an intramolecular hydrogen bond was found to be more than 10 kcal mol^{-1} higher in energy. Distances are given in angstroms (Å) and relative free energies ($\Delta\Delta G$) in kcal mol^{-1} (B3LYP-D3(BJ)/def2-TZVPP/IEF-PCM-(toluene)//B3LYP/6-31G(d)/IEF-PCM (toluene) (M06-2X/def2-TZVPP/IEF-PCM(toluene)//B3LYP/6-31G(d)/IEF-PCM (toluene)); O red, N blue, P orange.

group into close proximity to the partially negatively charged ester group (3.60 Å). Interestingly, the overlay of the structures along the chiral backbone reveals that the conformation within this chain remains identical in both transition states. Distortion/interaction analysis by the use of M06-2X/def2-TZVPP/IEF-PCM(toluene) shows that distortion is solely responsible for the discrimination of (*R*)-TS ($\Delta\Delta E^{\neq}_{dist} = 3.2$ kcal mol^{-1}), whereas the interactions in this transition state are in fact slightly more favorable ($\Delta\Delta E^{\neq}_{int} = -0.9$ kcal mol^{-1}).

In summary, we have elucidated the origins of stereoselectivity in the allene–enone (3+2) annulation reaction reported by Cowen and Miller. The enantiodetermining transition states that lead to both the major and the minor enantiomer are highly preorganized owing to an intermolecular hydrogen bond between the amide vicinal to the phosphonium ion and the substrate. Stabilization of the system is further enhanced by additional intermolecular hydrogen-bonding interactions between acidic C–H groups of the catalyst and the substrate. To enable these stabilizing interactions to occur, the reactant has to undergo significant distortion in the transition state leading to the minor enantiomer. A repulsive interaction between the carbamate carbonyl oxygen atom and the oxygen atom of the zwitterion is proposed to be largely responsible for the experimentally observed enantioselectivity. Owing to the structural similarities between the catalyst that we studied and other aminophosphine catalysts, our study should provide valuable insight into catalyst design for this and related reactions.

Experimental Section

Conformational searches were performed by using the OPLS-2005 force field in MacroModel 10.0.[12] All structures within 5 kcal mol^{-1} of the energetic minimum were subsequently optimized by using Gaussian 09[13] at the B3LYP[14]/6-31G(d) level of theory. Solvation by toluene was taken into account by using the integral equation formalism polarizable continuum model (IEF-PCM).[15] All optimized geometries were verified by frequency calculations as minima or transition structures (zero or a single imaginary frequency, respectively). Single-point energies, including empirical dispersion correction, were obtained by using B3LYP-D3(BJ)[16]/def2-TZVPP[17]/IEF-PCM and M06-2X[18]/def2-TZVPP/IEF-PCM. Entropic corrections to the free energies were calculated by using the Truhlar quasiharmonic approximation (vibrational frequencies lower than 100 cm^{-1} are set equal to 100 cm^{-1} to correct for the breakdown of the harmonic oscillator approximation for low frequencies).[19] GaussView 5.0[20] was used to generate input and visualize output structures. CYLview[21] and MacPyMOL[22] were used to render computed structures.

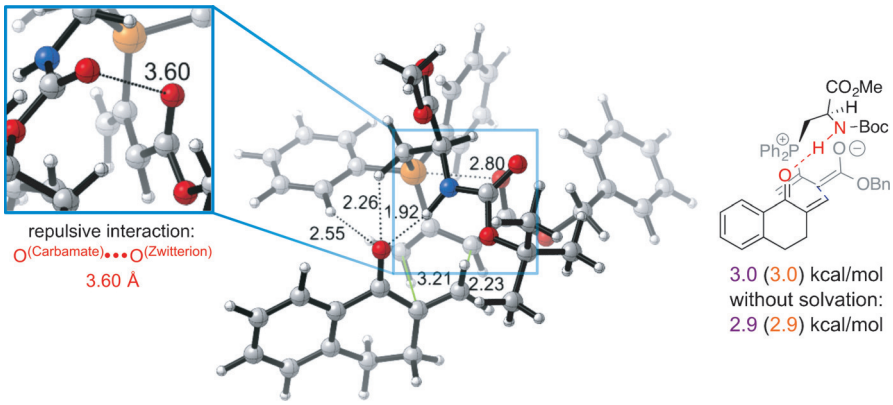

Figure 5. Transition state leading to the minor enantiomer. A repulsive interaction between the carbamate carbonyl oxygen atom and the oxygen atom of the zwitterion is proposed to be responsible for enantioselectivity. Distances are given in angstroms (Å) and relative free energies ($\Delta\Delta G$) in kcal mol^{-1} (B3LYP-D3(BJ)/def2-TZVPP/IEF-PCM(toluene)//B3LYP/6-31G(d)/IEF-PCM(toluene) (M06-2X/def2-TZVPP/IEF-PCM(toluene)//B3LYP/6-31G(d)/IEF-PCM(toluene)); O red, N blue, P orange.

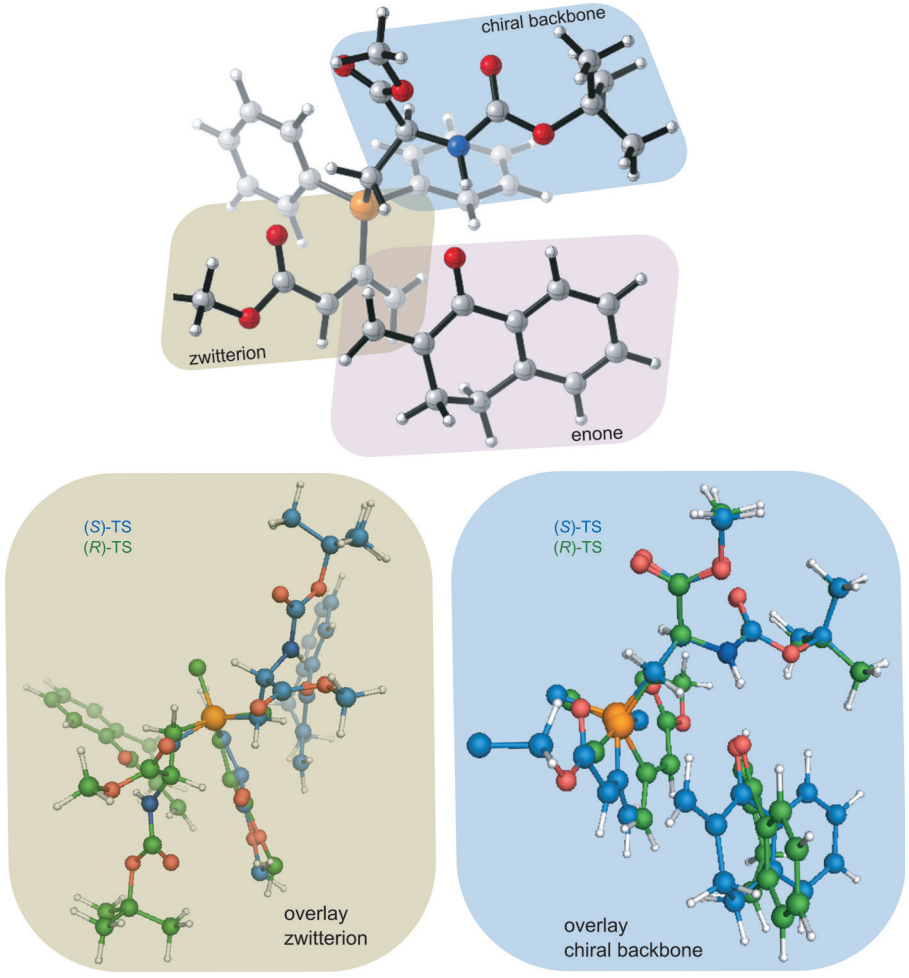

Figure 6. Overlay of the transition states leading to the major and the minor enantiomer along the zwitterion (left) and the chiral backbone (right). The blue structures correspond to the TS leading to the major enantiomer and the green structures to the TS leading to the minor enantiomer. O red, N blue, P orange.

Acknowledgements

We acknowledge generous financial support from the German Academic Exchange Service, DAAD (PRIME Fellowship to M.C.H.) and the US National Science Foundation (CHE-1361104). We thank the Deutsche Forschungsgemeinschaft Excellence Cluster EXC 1003 "Cells in Motion" for generous financial support. We thank Prof. Ohyun Kwon and Dr. Yu-hong Lam for helpful discussions.

Keywords: asymmetric catalysis · computational chemistry · conformational analysis · organocatalysis · phosphanes

How to cite: *Angew. Chem. Int. Ed.* **2016**, *55*, 2022–2027
Angew. Chem. **2016**, *128*, 2062–2067

[1] a) J. L. Methot, W. R. Roush, *Adv. Synth. Catal.* **2004**, *346*, 1035–1050; b) Z. Wang, X. Xu, O. Kwon, *Chem. Soc. Rev.* **2014**, *43*, 2927–2940.
[2] a) C. Zhang, X. Lu, *J. Org. Chem.* **1995**, *60*, 2906–2908; b) Z. Xu, X. Lu, *Tetrahedron Lett.* **1997**, *38*, 3461–3464.
[3] a) I. P. Andrews, O. Kwon, *Chem. Sci.* **2012**, *3*, 2510–2514; b) X. Han, F. Zhong, Y. Wang, Y. Lu, *Angew. Chem. Int. Ed.* **2012**, *51*, 767–770; *Angew. Chem.* **2012**, *124*, 791–794.
[4] B. J. Cowen, S. J. Miller, *J. Am. Chem. Soc.* **2007**, *129*, 10988–10989.
[5] For excellent reviews on the topic, see: a) Z. Chai, G. Zhao, *Catal. Sci. Technol.* **2012**, *2*, 29–41; b) L.-W. Xu, *ChemCatChem* **2013**, *5*, 2775–2784; c) B. J. Cowen, S. J. Miller, *Chem. Soc. Rev.* **2009**, *38*, 3102–3116; d) S. Yu, S. Ma, *Angew. Chem. Int. Ed.* **2012**, *51*, 3074–3112; *Angew. Chem.* **2012**, *124*, 3128–3167; e) Y. Xiao, Z. Sun, H. Guo, O. Kwon, *Beilstein J. Org. Chem.* **2014**, *10*, 2089–2121.
[6] For selected examples, see: a) Y. Q. Fang, E. N. Jacobsen, *J. Am. Chem. Soc.* **2008**, *130*, 5660–5661; b) H. Xiao, Z. Chai, C.-W. Zheng, Y.-Q. Yang, W. Liu, J.-K. Zhang, G. Zhao, *Angew. Chem. Int. Ed.* **2010**, *49*, 4467–4470; *Angew. Chem.* **2010**, *122*, 4569–4572; c) X. Han, Y. Wang, F. Zhong, Y. Lu, *J. Am. Chem. Soc.* **2011**, *133*, 1726–1729; d) F. Hu, Y. Wei, M. Shi, *Tetrahedron* **2012**, *68*, 7911–7919.
[7] a) E. Mercier, B. Fonovic, C. Henry, O. Kwon, T. Dudding, *Tetrahedron Lett.* **2007**, *48*, 3617–3620; b) X.-F. Zhu, C. E. Henry, O. Kwon, *J. Am. Chem. Soc.* **2007**, *129*, 6722–6723; c) Y. Xia, Y. Liang, Y. Chen, M. Wang, L. Jiao, F. Huang, S. Liu, Y. Li, Z.-X. Yu, *J. Am. Chem. Soc.* **2007**, *129*, 3470–3471; d) Y. Liang, S. Liu, Y. Xia, Y. Li, Z.-X. Yu, *Chem. Eur. J.* **2008**, *14*, 4361–4373; e) G.-T. Huang, T. Lankau, C.-H. Yu, *J. Org. Chem.* **2014**, *79*, 1700–1711.
[8] R. P. Gandhi, M. P. S. Ishar, *Magn. Reson. Chem.* **1991**, *29*, 671–674.
[9] Prof. O. Kwon has informed us that her group has seen in deuterium labeling experiments that even under anhydrous conditions the proton transfer is catalyzed by trace amounts of water.
[10] R. Lee, F. Zhong, B. Zheng, Y. Meng, Y. Lu, K.-W. Huang, *Org. Biomol. Chem.* **2013**, *11*, 4818–4824.
[11] T. Wang, Z. Yu, D. L. Hoon, K.-W. Huang, Y. Lan, Y. Lu, *Chem. Sci.* **2015**, *6*, 4912–4922.
[12] *MacroModel*, version 10.6, Schrödinger, LLC, New York, NY, **2014**.
[13] Gaussian 09, revision D.01, M. J. Frisch et al., Gaussian, Inc., Wallingford, CT, **2013**.
[14] a) S. H. Vosko, L. Wilk, M. Nusair, *Can. J. Phys.* **1980**, *58*, 1200–1211; b) C. Lee, W. Yang, R. G. Parr, *Phys. Rev. B* **1988**, *37*, 785–789; c) A. D. Becke, *J. Chem. Phys.* **1993**, *98*, 5648–5652; d) P. J. Stephens, F. J. Devlin, C. F. Chabalowski, M. J. Frisch, *J. Phys. Chem.* **1994**, *98*, 11623–11627.
[15] E. Cancès, B. Mennucci, J. Tomasi, *J. Chem. Phys.* **1997**, *107*, 3032–3041.
[16] a) S. Grimme, J. Antony, S. Ehrlich, H. Krieg, *J. Chem. Phys.* **2010**, *132*, 154104; b) S. Grimme, S. Ehrlich, L. Goerigk, *J. Comput. Chem.* **2011**, *32*, 1456–1465; c) E. R. Johnson, A. D. Becke, *J. Chem. Phys.* **2006**, *124*, 174104; d) E. R. Johnson, A. D. Becke, *J. Chem. Phys.* **2005**, *123*, 024101; e) L. Goerigk, S. Grimme, *Phys. Chem. Chem. Phys.* **2011**, *13*, 6670–6688.
[17] F. Weigend, R. Ahlrichs, *Phys. Chem. Chem. Phys.* **2005**, *7*, 3297–3305.
[18] Y. Zhao, D. Truhlar, *Theor. Chem. Acc.* **2008**, *120*, 215–241.
[19] a) R. F. Ribeiro, A. V. Marenich, C. J. Cramer, D. G. Truhlar, *J. Phys. Chem. B* **2011**, *115*, 14556–14562; b) Y. Zhao, D. G. Truhlar, *Phys. Chem. Chem. Phys.* **2008**, *10*, 2813–2818.
[20] R. Dennington, T. Keith, J. Millam, *GaussView*, version 5.0, Semichem Inc., Shawnee Mission, KS, **2009**.
[21] C. Y. Legault, *CYLview*, version 1.0b, Université de Sherbrooke, Sherbrooke, Québec, Canada, **2009**.
[22] *The PyMOL Molecular Graphics System*, version 1.3, Schrödinger, LLC, New York, NY, **2014**.

Received: September 24, 2015
Revised: November 25, 2015
Published online: January 6, 2016

